*lubricants*

MDPI

*Article*

# Enhanced Tribological Properties of Castor and Sesame Oil Mixture with Ascorbyl Palmitate for Boundary Lubrication

**Sandra Rojas-Osorio [1], Marco Ulises Negrete-Ríos [1], José E. Báez [2], María Teresa Hernández-Sierra [3] and Karla J. Moreno [1,4,*]**

[1] Doctoral Program in Engineering Sciences, Tecnológico Nacional de México/IT de Celaya, Celaya 38010, Mexico; d2403015@itcelaya.edu.mx (S.R.-O.); d2503006@celaya.tecnm.mx (M.U.N.-R.)
[2] Department of Chemistry, University of Guanajuato (UG), Guanajuato 36050, Mexico; jebaez@ugto.mx
[3] Automotive Systems Engineering Division, Tecnológico Nacional de México/ITS de Irapuato, Irapuato 36821, Mexico; teresa.hs@irapuato.tecnm.mx
[4] Mechanical Engineering Department, Tecnológico Nacional de México/IT de Celaya, Celaya 38010, Mexico
* Correspondence: karla.moreno@itcelaya.edu.mx; Tel.: +52-461-611-7575; Fax: +52-461-611-7878

**Abstract**

Vegetable oil blends significantly improve friction and wear performance compared to individual oils. However, the oxidizing nature of these blends remains a consistent challenge. Currently, both natural and synthetic antioxidants are recommended to address this issue. This study investigated the use of ascorbyl palmitate as a natural additive in a previously evaluated mixture of castor and sesame oils, focusing on its tribological performance in an AISI 4140/AISI 52100 tribopair. The chemical composition of the biolubricants was analyzed using Fourier-transform infrared spectroscopy (FTIR), while the physical properties such as density and kinematic viscosity were measured at various temperatures. To evaluate their suitability for tribological applications, their friction and wear performance were assessed using a ball-on-disk tribometer. The friction coefficient, coefficient of lubrication efficiency (CLE), and wear behavior (volume loss, wear rate, and wear mechanism) were analyzed. This study demonstrates a notable enhancement in the tribological properties of the binary mixture with varying ascorbyl palmitate concentrations (0.25, 0.5, and 0.75 wt.%). The addition of ascorbyl palmitate reduces wear by forming protective interfacial layers, resulting in a low friction coefficient of 0.07 and a 46% reduction in volume loss. Some concentrations of ascorbyl palmitate also mitigated the severity of the wear mechanism.

**Keywords:** antioxidant; ascorbyl palmitate; biolubricant; castor oil; sesame oil; oil mixture; friction; wear

Check for updates

Received: 15 May 2026
Revised: 26 June 2026
Accepted: 8 July 2026
Published: 9 July 2026

**Copyright:** © 2026 by the authors. Licensee MDPI, Basel, Switzerland. This article is an open access article distributed under the terms and conditions of the Creative Commons Attribution (CC BY) license.

## 1. Introduction

The growing demand for sustainable technologies, along with stricter environmental laws, has spurred the development of biolubricants as alternatives to petroleum-based lubricants [1]. Vegetable oils have attracted considerable attention because of their high lubricity, biodegradability, and low toxicity; however, their use in demanding applications is still limited by their relatively poor oxidative stability and inadequate performance under severe contact conditions, especially in boundary lubrication regimes [1,2].

Among vegetable oils, castor oil is notable for its ricinoleic acid content, which gives it high intrinsic viscosity, excellent lubricity, and a strong affinity for metallic surfaces. Additionally, as a non-edible oil, its use does not compete with food resources. In comparison, sesame oil offers improved oxidative stability, a high flash point, and favorable

low-temperature properties. Therefore, combining both oils in an oil mixture offers a promising approach to balance lubricity and thermal stability, resulting in a more robust base lubricant than either oil alone [1,3].

The importance of optimizing vegetable oil mixtures has been previously demonstrated in the tribological system AISI 52100/8620 steel under green oil lubrication, where binary mixtures of vegetable oils significantly improved friction and wear behavior compared to single oils. An optimized castor–sesame mixture reduced the coefficient of friction by approximately 10%, while other combinations achieved wear reductions of up to 81% [3]. These findings highlight that tribological performance depends not only on the base oil but also on the proper selection of mixture composition.

Lubricants generally consist of a base oil that can be neat mineral, synthetic or bio-based oil, or even oil mixtures and additives, substances incorporated to enhance certain properties or characteristics. Additives can be classified into three complementary categories: by working function, by working site, and by working mechanism [4]. By working function, they act as tribo-improvers (friction modifiers, anti-wear agents, extreme pressure additives), rheo-improvers (viscosity modifiers, pour point depressants), maintainers (antioxidants, detergents, dispersants, corrosion inhibitors, anti-foam agents, demulsifiers), or auxiliaries for specific purposes. By working site, they operate either at interfaces (solid–liquid or gas–liquid boundaries) or within the bulk phase of the lubricant. Finally, by working mechanism, they function through chemical reactions (irreversible tribo-chemical films, oxidation prevention) or physical processes (nanoparticles, viscosity control). Some additives have functions that span multiple categories, meaning they combine properties from two or even all three groups [4].

In turn, lubricant additives can be broadly divided into natural and synthetic types, depending on their origin and method of production. Natural additives are derived from renewable resources such as plants, animals, or naturally occurring minerals, while synthetic additives are chemically engineered compounds for superior performance under extreme conditions [5]. In practice, lubricant formulations mostly use synthetic additives or a combination of them; however, to develop fully biodegradable lubricants, natural alternatives must be chosen to strike a balance between performance and environmental impact.

Ascorbic acid has emerged as a promising candidate due to its antioxidant properties [6] and high polarity, which promote strong interactions with metallic surfaces. It is a naturally occurring organic compound, widely found in fruits and vegetables, and produced industrially through fermentation processes, which ensures broad availability and a low environmental impact [7]. However, ascorbic acid is hydrophilic and is characterized by having very low solubility in oils. Ascorbyl palmitate is composed of an ascorbic acid core attached to a flexible alkyl chain (palmitic acid) so that it is lipophilic. From a molecular standpoint, the amphiphilic structure of ascorbyl palmitate, combining the antioxidant core of ascorbic acid with a long lipophilic chain, facilitates its integration into lipid environments and adsorption at oil–metal interfaces, thereby contributing to the formation of more stable protective layers in tribological systems. Along with its biodegradability, these features make it an attractive option for use as an additive in the development of sustainable lubrication systems in various oil base stocks such as polyalphaolefin (PAO4), soybean oil, castor oil, and rubber seed oil [8–12].

Considering previous studies on the use of ascorbyl palmitate as a lubricant additive, most have focused on evaluating the ability of antioxidants to delay oil oxidation [1,3–6]. Some have analyzed how additives affect the viscosity and viscoelastic properties of lubricating oil or grease [1,3,5] or have evaluated certain physicochemical properties and corrosion [3]. Therefore, its application in tribological systems remains limited compared to conventional additives. The study by Long et al. (2022) [8] has shown that ascorbyl

palmitate can reduce friction and wear through mechanisms associated with adsorption and the formation of protective boundary films in PAO. Its ascorbic acid core allows for robust chemical adsorption on steel surfaces by forming bidentate and monodentate C-O-Fe bonds. This mechanism enables a surface coverage rate near 100%, providing a protective "liquid" monolayer that can survive extreme pressures (up to 2.11 GPa).

Under a boundary lubrication regime, the lubricant film thickness becomes comparable to or even smaller than the surface roughness of the contacting materials, promoting direct asperity interactions. Consequently, tribological behavior is no longer governed by bulk lubricant properties, such as viscosity, but rather by interfacial phenomena, including molecular adsorption and tribochemical reactions [13,14]. Therefore, the effectiveness of a lubricant in such systems strongly depends on its ability to modify the solid–solid interface during sliding.

In tribological contacts, particularly when high loads are combined with elevated temperatures and relatively low sliding speeds, the lubricant's ability to form a full hydrodynamic film is limited. As a result, the lubrication regime tends to shift toward boundary lubrication conditions [14]. For example, the tribological system of AISI 52100 against AISI 4140 has significant industrial importance. AISI 52100 is commonly used in rolling elements due to its high hardness and wear resistance, while AISI 4140 is frequently employed in shafts, gears, cams, and other heavily loaded mechanical parts. These materials often operate under contact pressures of hundreds of MPa, making them suitable systems for evaluating lubricant performance under severe conditions [15].

Based on these considerations, the present study aims to evaluate the tribological performance of a binary mixture of castor and sesame oils containing different concentrations of ascorbyl palmitate under controlled conditions using an AISI 52100/AISI 4140 contact. Emphasis is placed on identifying the optimal additive concentration and correlating the observed friction and wear behavior with physicochemical properties, lubrication regime, and underlying wear mechanisms. In this context, this work seeks to contribute to the development of high-performance, biodegradable lubricants while providing insight into the role of lubricant composition and interfacial phenomena in steel–steel contacts operating under severe conditions.

## 2. Materials and Methods

### 2.1. Additives

Ascorbic acid 6-palmitate, also known as ascorbyl palmitate, was used as a natural additive in the formulation of biolubricants. This compound (CAS number 137-66-6) (Sigma-Aldrich, St. Louis, MO, USA), was selected because of its ability to inhibit oxidation processes in organic systems through free radical scavenging mechanisms, which could help improve the chemical stability of biolubricants [16]. Additionally, the presence of polar functional groups in its molecular structure may facilitate interactions with metal surfaces, potentially contributing to the formation of protective films during tribological contact [16].

### 2.2. Lubricant Formulation

The biolubricants evaluated in this study were formulated from a binary mixture of castor oil (CO) and sesame oil (SO) sourced from a local supplier. They were selected due to their previously reported tribological performance in the literature when both oils are used in combination [3]. It has been reported that a CO/SO mixture with a castor oil molar fraction close to XCO = 0.7484 exhibits superior tribological behavior compared to the individual oils, evidenced by a reduction in the coefficient of friction and wear during sliding contact tests. This behavior has been attributed to the synergy between both oils, where the high polarity of castor oil promotes adsorption on the metallic surface and the

formation of a lubricating film, while sesame oil contributes to improving the fluidity of the system and the stability of lubrication [3].

Based on these findings, a base oil called COSO was prepared using a castor oil molar fraction of XCO = 0.7484, with the remaining fraction consisting of sesame oil. Then, ascorbyl palmitate was incorporated as an additive at different concentrations to evaluate its effect on the tribological behavior. The biolubricants were designated as CSA 1, CSA 2, and CSA 3, corresponding to formulations containing 0.25, 0.5, and 0.75 wt.% of ascorbyl palmitate, respectively. Each formulation was prepared individually by stirring at 525 rpm with a magnetic stirrer for 10 min at room temperature using a 250 mL borosilicate glass beaker. The required amount of ascorbyl palmitate was added directly to the COSO base mixture and dispersed by magnetic stirring under the previously described conditions.

To evaluate the physical stability of the biolubricant formulations, particularly regarding sedimentation and phase separation, samples of each lubricant were subjected to centrifugation at 6000 rpm for periods of 10 and 30 min. Figure 1 exhibits the appearance of the formulated biolubricants, both freshly prepared and after vigorous agitation in an IKA mini G centrifuge (IKA-Werke, Staufen, Baden-Württemberg, Germany). Under these conditions, no evidence of sedimentation, precipitation, or additive separation was observed, indicating that the formulations maintained homogeneity and structural integrity. The absence of phase separation under high centrifugal stress suggests that the ascorbyl palmitate was well incorporated into the oil blend and that the biolubricants exhibit good physical stability.

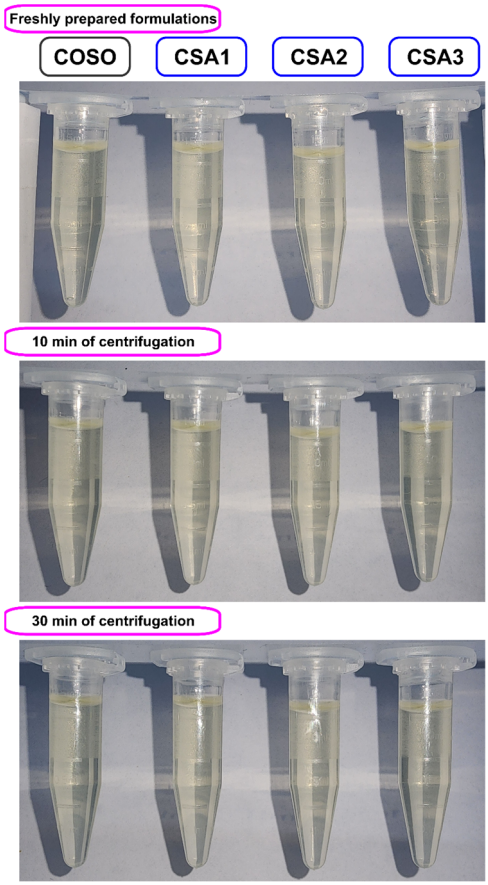


**Figure 1.** Appearance of the formulated, freshly prepared biolubricants and samples after vigorous agitation.

### 2.3. Chemical Characterization of the Biolubricants

The chemical composition of the formulated biolubricants was analyzed using Fourier-transform infrared spectroscopy with attenuated total reflectance (ATR-FTIR) on a Spectrum 100 spectrometer (PerkinElmer, Waltham, MA, USA). The system features a $LiTaO_3$ detector, a KBr beam splitter, and an ATR accessory with a ZnSe crystal, suitable for direct analysis of liquid samples. Spectra were obtained in the 4000–500 $cm^{-1}$ wavenumber range with a spectral resolution of 4 $cm^{-1}$ and three scans for each sample. For each measurement, a small amount of the bio-lubricant was placed directly on the ATR crystal, ensuring good contact between the sample and the crystal surface during spectral collection. The obtained spectra were used to identify the characteristic functional groups of the vegetable oils in the formulations and to assess possible spectral changes associated with the incorporation of ascorbyl palmitate into the biolubricants.

### 2.4. Physical Characterization

The physical properties of the biolubricants were evaluated by measuring density and kinematic viscosity at different temperatures, parameters commonly used to assess the suitability of vegetable oils for tribological applications. The density of the formulations was determined using the pycnometer method at 25, 40, and 100 °C, following procedures described for liquid density measurement with a pycnometer [17]. For each measurement, the pycnometer was filled with the respective sample and weighed using an OHAUS Explorer Pro analytical balance (Ohaus Corp., Parsippany, NJ, USA). Measurements were taken once thermal equilibrium was reached at each temperature.

The kinematic viscosity of the biolubricants was measured at 25, 40, and 100 °C using glass Oswald capillary viscometers (Cannon Instrument Company, State College, PA, USA). Viscometers of sizes 200 and 350 were used depending on the viscosity range of the samples. During each measurement, the samples were kept at the test temperature until thermal equilibrium was reached. The flow time of the lubricant through the capillary was recorded and used to calculate the corresponding viscosity, following standardized procedures for determining kinematic viscosity [18]. Finally, the density and viscosity values obtained at different temperatures were fitted using an Arrhenius-type relationship to describe the temperature dependence of these properties [19].

### 2.5. Contact Angle of the Biolubricants

In order to quantify the wettability of the biolubricants and provide information about the interaction between cohesive and adhesive forces, the static contact angle of the biolubricants was determined by the sessile drop technique. For this purpose, 6 µL droplets of each lubricant were carefully placed on an AISI 4140 steel surface with a precision micropipette. The steel discs had the same roughness as for the tribological tests and were cleaned with methanol before the experiments to ensure the reliability of the results. The physical behavior of each droplet was recorded using a Keyence VHX-970F digital microscope (Keyence, Osaka, Japan) by side-view videos at 30×. Images were extracted immediately after deposition (t = 0 s) and after 75 s to evaluate the time-dependent wetting behavior, in accordance with established methodological guidelines for contact angle measurements [20,21]. The droplet profiles were mathematically adjusted to a circumscribed circle using the standard circle equation, from which the slope of the tangent at the solid–liquid interface was derived. The contact angle (φ) was then calculated through a trigonometric relation, following procedures commonly reported in the literature [22].

### 2.6. The Lubrication Regime Estimation

To estimate the lubrication regime during the tribological tests, the film thickness ratio ($\lambda_c$) was determined as the ratio of the central lubricant film thickness ($h_c$) to the combined roughness on the contacting surfaces using Equation (1), where $R_1$ and $R_2$ represent the root mean square roughness of the disk and ball surfaces, respectively. Then, the lubrication regime was classified according to the value of $\lambda_c$, considering boundary lubrication when $\lambda_c < 1$, mixed lubrication when $1 < \lambda_c < 3$, and elastohydrodynamic lubrication when $\lambda_c > 3$ [23,24].

$$\lambda c = \frac{h_c}{\sqrt{R_1^2 + R_2^2}} \tag{1}$$

The central lubricant film thickness ($h_c$), as shown in Figure 2, was then estimated using mathematical Equation (2), proposed by Hamrock and Dowson [23,24] for elastohydrodynamic contacts in sphere/flat configurations.

$$h_c = HcR = \left[2.69U^{0.67}G^{0.53}W^{-0.067}\left(1 - 0.061e^{-0.73k}\right)\right]R \tag{2}$$

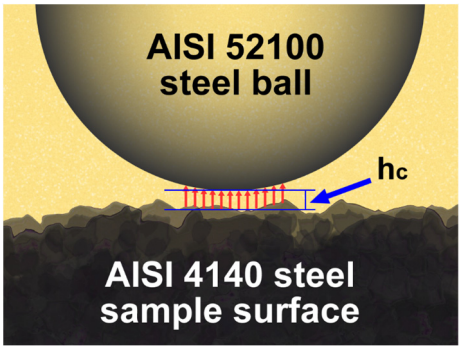


**Figure 2.** Scheme of the central lubricant film thickness.

In Equation (2), $R$ is the effective contact radius, $U$, $G$, and $W$ are the dimensionless parameters of speed, material, and load, respectively, and $k$ is the ellipticity parameter. The dimensionless parameters were calculated with Equations (3)–(5):

$$U = \eta_0 V_r / \left(E' R_x\right) \tag{3}$$

$$G = E' \alpha_p \tag{4}$$

$$W = F / \left(E' R_x^2\right) \tag{5}$$

In the above equations, $\eta_0$ represents the viscosity at atmospheric pressure, $V_r$ denotes the relative velocity ($V_r = V_{disc} + V_{pin})/2$), $E'$ corresponds to the effective elastic modulus of the contacting bodies in the AISI 4140/AISI 52100 steel contact, $\alpha_p$ represents the pressure–viscosity coefficient, and $F$ represents the normal load.

In this study, the pressure–viscosity coefficient ($\alpha_p$) was calculated from the fluids' thermodynamic parameters using Equation (6), where $\beta$ is the compressibility coefficient, $S_{v/T}$ is the slope of the graph of the logarithm of viscosity vs. the reciprocal of temperature, $\alpha_T$ is the thermal expansivity coefficient, and $T$ is the absolute temperature.

$$\alpha_P = -\frac{\beta(S_{v/T})}{2\alpha_T T^2} \tag{6}$$

The thermal expansivity coefficient ($\alpha_T$), as shown in Equation (7), was estimated using thermodynamic relationships that relate density changes with temperature, where $\rho$ is the lubricant density, and $\Delta\rho/\Delta T$ indicates how density changes with temperature.

$$\alpha_T = (1/\rho)(\Delta\rho/\Delta T) \tag{7}$$

*2.7. Tribological Tests*

The tribological performance of the formulated biolubricants was assessed using a TRB tribometer (CSM Instruments, Needham, MA, USA) operating in a ball-on-disk configuration, following the guidelines established in the ASTM G99-23 standard [25]. The tests used an annealed AISI 4140 steel disk as the substrate and an AISI 52100 steel ball as the counterpart. The disk had a diameter of 25.4 mm and a thickness of 5 mm, while the ball measured 3 mm in diameter. The hardness of the AISI 4140 steel was measured with a Vickers–Knoop microhardness tester (MetroTec Quality Control Instruments, Lezo, Spain), resulting in an average of 189 HV. The AISI 52100 steel ball had a hardness of 697 HV, based on the specifications from the supplier (Anton Paar, Graz, Austria). The mechanical properties for these materials include a tensile strength of 850 MPa for AISI 4140 steel and approximately 2 GPa for AISI 52100 steel, according to the material suppliers. The initial surface roughness was measured using contact profilometry with a Mitutoyo SJ-400 roughness tester (Mitutoyo Corp., Kawasaki, Japan), resulting in an average Ra value of 0.03 µm. At least five measurements were taken on each surface to verify the consistency of the surface topography prior to the tribological tests.

The experiments were conducted with a wear track radius of 2 mm, a linear sliding speed of 2.5 cm/s, and a rotation frequency of 2 Hz to complete 30,000 sliding cycles. Under these conditions, a mean contact pressure (Pm) of approximately 500 MPa was estimated using Hertzian contact theory for a sphere-flat contact setup [26]. All tests were performed at a constant temperature of 100 °C, using 60 mL of each formulated lubricant. During the tests, the friction force was continuously recorded using the Tribox 4.5R software with the tribometer data acquisition system, enabling the calculation of the relevant coefficient of friction. To ensure reproducibility, three tribological tests were conducted for each lubricant system. The schematic illustration in Figure 3 shows the experimental setup of the tribometer, the data acquisition system, and the relative positioning of the disk and ball during the test.

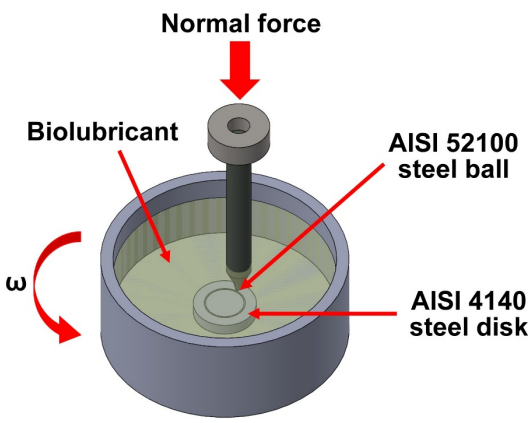


**Figure 3.** Configuration of a tribological test on a ball-on-disk TRB tribometer.

The lubrication efficiency coefficient (CLE) was calculated to evaluate the lubrication performance of the tested formulations, using the method from Trzepieciński et al. [27]. This coefficient assesses how well the lubricant reduces friction compared to dry sliding.

The CLE parameter indicates the relative reduction in the coefficient of friction, with higher values showing greater lubrication efficiency [27].

The wear tracks on the disk surfaces were examined using an optical microscope Carl Zeiss Axio Imager A1m (ZEISS, Göttingen, Germany). From the images obtained, the wear track width (WTW) was measured at various points along the wear path using microscope analysis software. The average WTW was then used to estimate the volume loss of material (V), based on the ball-on-disk contact geometry described in ASTM G99-23 [25]. The wear volume of the disk was calculated using the geometric relationship of the spherical segment, expressed by Equation (8), where R is the wear track radius, d is the average wear track width, and r is the radius of the ball. Based on the volume loss, the wear rate (K) was calculated according to Equation (9), where F is the applied normal load, and D is the total sliding distance [25].

$$V = (\pi R d^3)/6r \tag{8}$$

$$K = V/FD \tag{9}$$

The 2.5D surface topography maps of the worn surface were created using the microscope software ZEN 2012 SP2 BLUE, provided by the supplier. Additionally, the roughness profile of the wear track cross-section was measured by contact profilometry with a Mitutoyo SJ-400 roughness tester (Mitutoyo Corp., Kawasaki, Japan) to confirm the WTW measurements obtained from optical microscopy.

Finally, the wear mechanisms were studied through the morphological observation of the wear tracks using optical microscopy. The classification of the observed wear modes was based on criteria established by K. Kato [28], which relies on identifying characteristic surface features in the two-dimensional images of the worn surfaces.

### *2.8. Thermal and Oxidation Behavior*

In order to explore the antioxidant potential of ascorbyl palmitate as an additive, samples of 3 ± 0.5 mg COSO and CSA 2 were analyzed by thermogravimetric analysis (TGA) and differential scanning calorimetry (DSC) as representatives. For this study, SDT Q600 V20.9 Build 20 (TA Instruments, New Castle, DE, USA) with a DSC-TGA Standard module was employed. Samples were placed in open aluminum pans under an airflow of 50 mL/min at ambient pressure. The heating rate was set at 10 °C/min, covering a temperature range from 30 °C to 500 °C. The antioxidant effectiveness of ascorbyl palmitate was determined by the oxidation onset temperature (OOT) of biolubricants, which is identified as the onset of the exothermic reaction and recorded and measured by extrapolating the onset temperature in a DSC graph.

## 3. Results

### *3.1. Chemical Characterization of the Biolubricants*

The ATR-FTIR spectra of the elements and the formulated biolubricants are shown in Figure 4. Figure 4a shows the FTIR spectra of ascorbyl palmitate and the two vegetable oils used, which agree with the literature [24,29,30]. The ascorbyl palmitate spectrum exhibited a composite band at about 3464 $cm^{-1}$ due to the hydroxyl stretching; two strong bands at 2914 $cm^{-1}$ and 2849 $cm^{-1}$ corresponding to $CH_2$ asymmetric and symmetric stretching vibrations, respectively; an intense band at around 1728 $cm^{-1}$ that is the result of the stretching vibration of the ester carbonyl C=O group; a small band at 1633 $cm^{-1}$ that is of double-bond C=C in ascorbic acid; and several bands in the 1500–1000 $cm^{-1}$ region related to C-O and C-O-C functional groups in the fatty acid [30,31]. The vegetable oil spectra show the same features as the stretching vibrations of aliphatic C-H bonds in the 2800–2950 $cm^{-1}$ region, a strong absorption band attributed to the ester carbonyl (C=O)

group around 1728 $cm^{-1}$, and a similar fingerprint region due to the fatty acid nature. Additionally, the castor oil spectrum shows a broad band at about 3430 $cm^{-1}$ belonging to vibrations of the O-H group due to its unique ricinoleic fatty acid content.

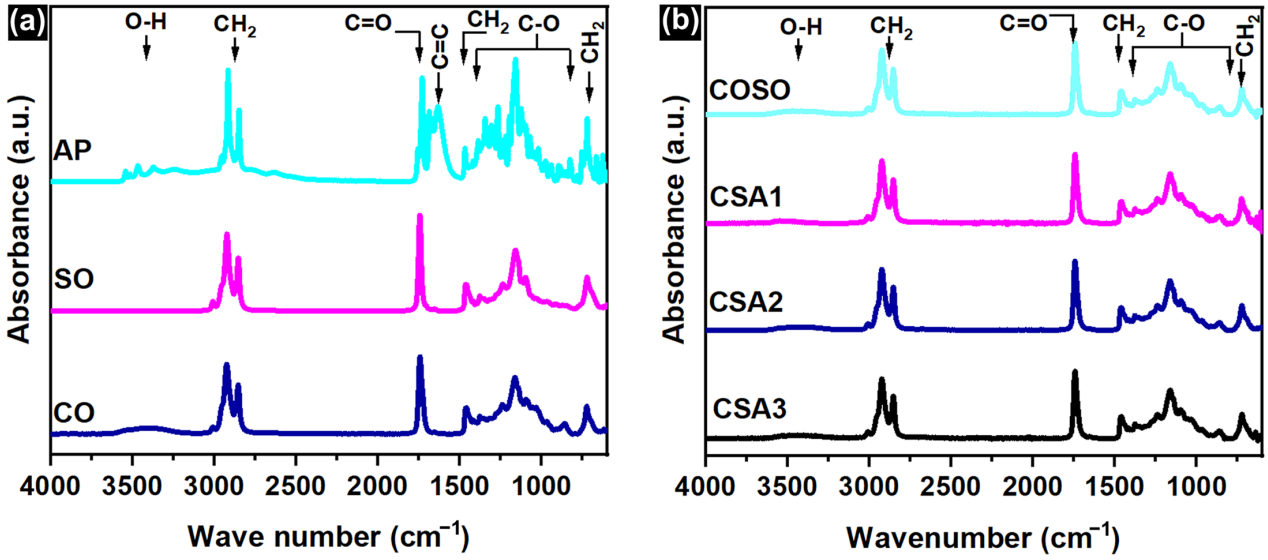


**Figure 4.** ATR-FTIR spectra of (**a**) compounds and (**b**) formulated biolubricants.

Figure 4a exhibits the spectra of biolubricant formulations. It can be observed that they are the typical signals of the vegetable oil nature. The addition of ascorbyl palmitate at the studied concentrations did not produce new absorption bands or noticeable shifts in the positions of the main functional groups. Minor variations in the C-H stretching region were observed; however, these differences were not considered significant.

### *3.2. Physical Characterization*

The density and kinematic viscosity of the formulated biolubricants as a function of temperature are shown in Figure 5. Between 25 and 70 °C, differences between formulations are minimal; however, above 70 °C, the base formulation (COSO) shows slightly higher density values. This suggests that the addition of the additive does not significantly influence the system's volumetric properties. The kinematic viscosity of all formulations shows a strong dependence on temperature, decreasing exponentially as temperature increases, which is characteristic of lubricants. At 40 °C, viscosity values are around 140 cSt, while at 100 °C, they decrease to approximately 14 cSt. The differences between the base formulation and the ascorbyl palmitate-containing formulations are small, indicating that these amounts of additive do not significantly modify the rheological behavior of the lubricant.

From a tribological perspective, the small variation in viscosity among formulations indicates that any possible differences in friction and wear behavior should not be attributed to changes in bulk flow properties but rather to interfacial phenomena such as additive adsorption or tribochemical interactions during sliding [8,32]. In lubricated systems operating under concentrated contact conditions, like those found in loaded mechanical components, pressures typically range from 0.1 to 0.5 GPa, where lubricant behavior is influenced by its viscosity and pressure–viscosity response [23,33]. In this context, the viscosity range observed in this study aligns with lubricants used in applications subjected to moderate pressures within this interval, such as mechanical transmission parts, hydraulic components, and lubricated contacts in industrial machinery, where different lubrication regimes can develop depending on operating conditions [23,33,34]. Under these conditions, lubri-

cant viscosity and its temperature dependence are crucial for film formation and stability. However, since viscosity differences between formulations are minimal, any variation in tribological performance should be analyzed based on interfacial phenomena occurring at the lubricant–surface interface [35].

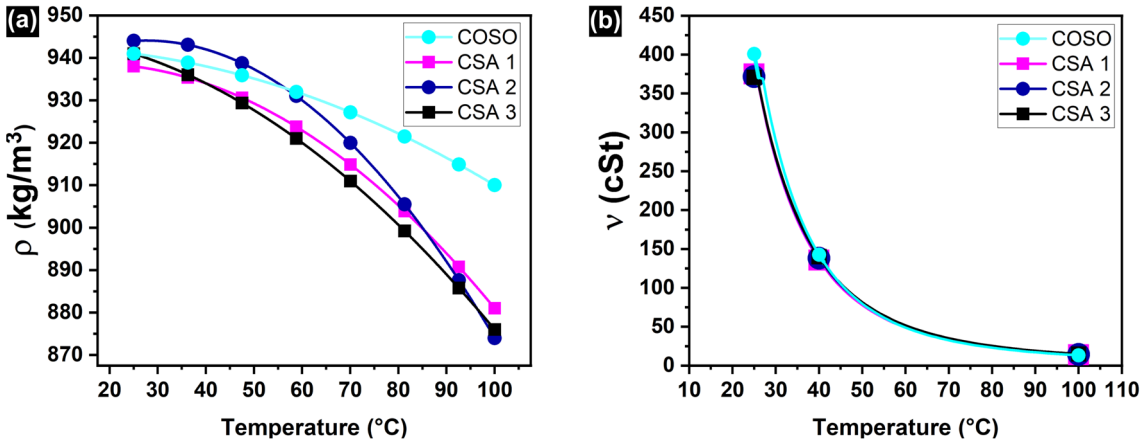


**Figure 5.** (**a**) Density and (**b**) kinematic viscosity of the biolubricants as a function of temperature.

### *3.3. Contact Angle of Biolubricants*

The contact angle results of biolubricants as soon as deposition and after 75 s are shown in Figure 6. It can be observed that there are clear differences between the base oil (COSO) and the formulations containing ascorbyl palmitate. Initially, COSO exhibited a lower contact angle (49.4°) compared to the CSA samples (54.6–57.0°), indicating greater wettability at time zero and lower cohesion. Nevertheless, the time-dependent behavior shows the opposite trend: COSO decreased moderately ($\Delta\varphi$ = 20.3°), while CSA formulations underwent much sharper reductions ($\Delta\varphi$ = 37.1–39.8°). Over time, the lubricants containing ascorbyl palmitate spread more across the surfaces, exhibiting a greater decrease in contact angle. This behavior could be explained by the polar nature of ascorbyl palmitate, which migrated toward the interface, enhancing surface adsorption, reducing surface tension, and consequently lowering the contact angle. This dynamic wetting behavior suggests that the incorporation of ascorbyl palmitate promotes stronger interfacial interactions and improved spreading capacity. Such enhanced wettability is critical for boundary lubrication, as it facilitates better film formation and protection of metallic surfaces.

### *3.4. The Lubrication Regime Estimation*

The values of the pressure–viscosity coefficient ($\alpha_p$), central film thickness ($h_c$), and lambda parameter ($\lambda_c$) for the different formulations are shown in Table 1. The results indicate that $h_c$ varies from 2.6 to 4.1 nm, while $\lambda_c$ stays between $1.33 \times 10^{-2}$ and $2.15 \times 10^{-2}$. Therefore, all formulations clearly operate in the boundary lubrication regime, where surface separation is limited to a few molecular layers and the tribological response is mainly driven by interfacial phenomena such as adsorption and tribochemistry [36–38]. Although the lambda values determined in this work are very low, they agree with published deterministic experiments and numerical simulations that report very low lambda regimes [39]. In fact, Zhu and Wang [39] concluded that if boundary lubrication is specified as the condition in which the contact surface supports more than 90% of the load, the associated $\lambda$ typically lies below about 0.01–0.05.

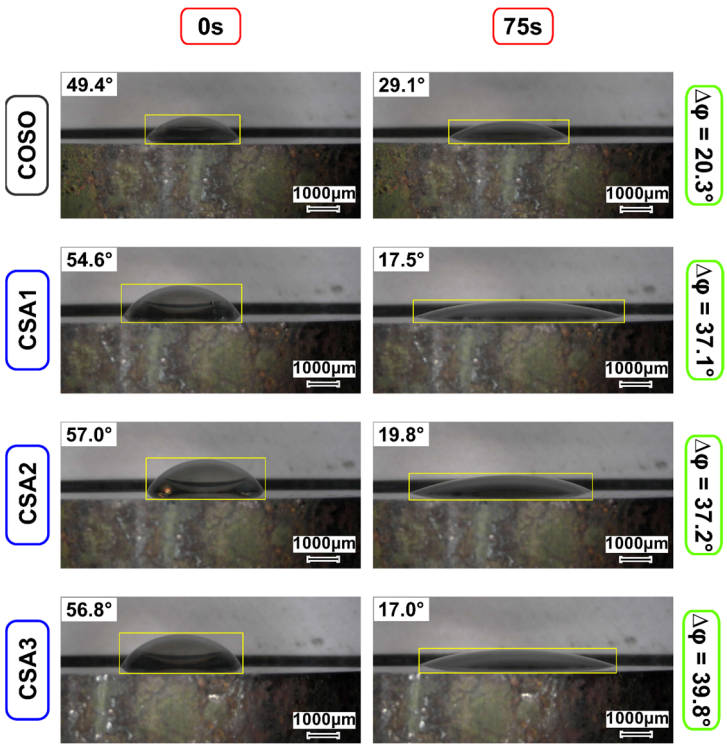


**Figure 6.** Contact angle behavior of biolubricants immediately after deposition and after 75 s.

**Table 1.** Lubrication regime parameters for biolubricants.

| Lubricant | $\alpha_p$ ($\times 10^{-8}$ Pa$^{-1}$) | $h_c$ (nm) | $\lambda_c$ ($\times 10^{-2}$) | Lubrication Regime |
|---|---|---|---|---|
| COSO | 3.65 | 4.1 | 2.15 | Boundary |
| CSA 1 | 1.73 | 2.9 | 1.48 | |
| CSA 2 | 1.35 | 2.6 | 1.33 | |
| CSA 3 | 1.55 | 2.8 | 1.46 | |

From this perspective, the fact that the base formulation shows the highest $\alpha_p$ and, consequently, the greatest film thickness does not necessarily mean improved tribological performance. Although a higher pressure–viscosity response encourages an increase in film thickness, the values remain in the nanometer range and are therefore insufficient to fully separate the surfaces. As a result, variations in $\alpha_p$ among formulations only lead to minor changes in $h_c$ and do not change the lubrication regime [23,36].

This interpretation aligns with classical tribology literature, where boundary lubrication is characterized by film thicknesses of only a few nanometers and where friction and wear are mainly influenced by adsorbed layers and tribochemical reactions [36–38]. In vegetable oil-based systems, it has been reported that polar additives improve tribological performance by forming protective interfacial films. Specifically, Moreno et al. [35] observed better friction–wear behavior in castor oil with natural additives due to interfacial interactions. Similar findings have been reported for biolubricants and friction modifiers, where the additive's effectiveness depends on its ability to adsorb onto the surface and form boundary films [36,37].

The film thickness values obtained in this study are therefore consistent with boundary lubrication conditions typically encountered in high-load, low-speed contacts and elevated temperatures, where lubricant viscosity decreases and the formation of a full hydrodynamic film is hindered [23]. Such conditions are commonly found in engineering components such as gears, rolling element bearings, piston rings, cams, and hydraulic elements operating under severe or transient conditions in which boundary lubrication may dominate [36,37].

### 3.5. Friction Behavior and Lubrication Efficiency

The evolution of the kinetic friction coefficient ($\mu_k$) as a function of the number of cycles for different formulations is shown in Figure 7, while the average $\mu_k$ values, the number of cycles needed to reach stability, and the coefficient of lubrication efficiency (CLE) are summarized in Table 2. Overall, all formulations show relatively stable behavior during the test; however, clear differences appear in both the magnitude of the $\mu_k$ and the number of cycles required to reach steady-state conditions.

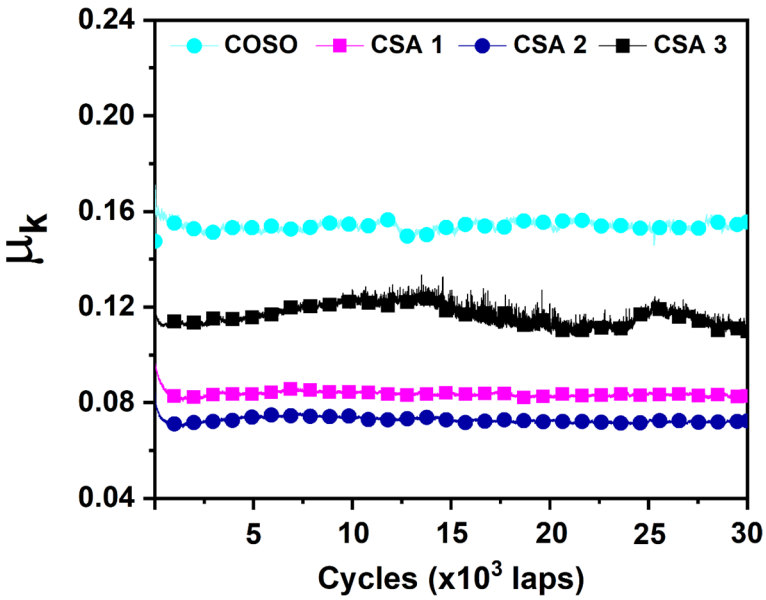


**Figure 7.** Kinetic friction coefficient ($\mu_k$) behavior for biolubricants.

**Table 2.** Summary of tribological performance parameters: stabilization cycles, steady-state $\mu_k$, and lubrication efficiency (CLE) of biolubricants.

| Lubricant | Cycles to Steady State ($\times 10^3$) | Steady State, $\mu_k$ | CLE (%) [a] |
|---|---|---|---|
| COSO | 15 | 0.15 | 75 |
| CSA 1 | 5 | 0.08 | 86 |
| CSA 2 | 5 | 0.07 | 88 |
| CSA 3 | 15 | 0.11 | 81 |

[a] CLE values were derived from the dry reference condition of the tribosystem under investigation ($\mu_k$ = 0.61).

Formulations with 0.25 and 0.50 wt.% ascorbyl palmitate reach steady-state conditions at around 5000 cycles, while CSA 3 and the base formulation take nearly 15,000 cycles. This indicates that a concentration of 0.5% or less of the additive promotes faster stabilization of the tribological contact, likely due to more effective interaction between the additive and metallic surfaces during the early stages of sliding.

Regarding the magnitude of friction, adding ascorbyl palmitate significantly reduces $\mu_k$ compared to the base formulation. COSO has an average $\mu_k$ of about 0.15, while CSA 1 and CSA 2 reach approximately 0.08 and 0.07, respectively. Although CSA 3 shows a higher $\mu_k$ than CSA 1 and CSA 2, it still improves over the base lubricant. This suggests that the effect of ascorbyl palmitate is not linear with concentration, although all formulations with additives perform better tribologically than COSO.

The CLE results support this trend, with CSA 2 showing the highest efficiency, followed by CSA 1 and CSA 3, while COSO displays the lowest value. This pattern confirms the presence of an optimal additive concentration where friction reduction is maximized. Similar patterns have been observed for polar and natural additives, where intermediate

concentrations improve tribological performance, but excessive concentrations can lead to surface saturation or the formation of less ordered adsorbed layers, thus decreasing their effectiveness [6,40].

From a molecular perspective, the behavior of ascorbyl palmitate can be explained by its highly polar nature and multiple hydroxyl groups, which enhance strong interactions with metallic surfaces. Unlike typical additives such as ZDDP, which are amphiphilic, ascorbyl palmitate can effectively adsorb onto surfaces, thereby facilitating the formation of a protective layer [6,41]. Previous studies have indicated that the adsorption density of polar molecules at the interface is directly linked to friction reduction, as increased surface coverage results in lower sliding resistance [32]. Additionally, it has been reported that the polarity of the system substantially affects additive adsorption and the formation of protective films on metallic surfaces [42] and that molecules with multiple adsorption sites tend to form more stable and resilient interfacial layers under load [43].

Under these circumstances, the improved performance observed for CSA 1 and CSA 2 may be due to more effective surface coverage promoted by ascorbyl palmitate. However, at higher concentrations, surface saturation or the formation of less-organized interfacial layers could limit the additive's effectiveness, aligning with the experimentally observed decrease in performance.

The notable decrease in CLE observed for CSA 1 and CSA 2 indicates their potential application in mechanical systems using AISI 52100-AISI 4140 tribological pairs, commonly found in components like rolling bearings, control valves, and precision machinery. Under contact conditions around 500 MPa, these systems operate within the elastic regime for both materials, considering AISI 4140′s hardness and mechanical resistance [36,44].

In this context, reducing friction can help lower tangential stresses at the contact interface, which is important in applications where surface fatigue is a primary wear mechanism. This aligns with design guidelines for moderately loaded mechanical contacts, where using materials with different hardness levels enables better distribution of stress and enhances tribological performance [36,44].

### *3.6. Wear Behavior Analysis*

The wear behavior of the different formulations is shown in Figures 8 and 9, which display the 2.5D surface topographies, cross-sectional profiles of the wear tracks, and corresponding optical micrographs. The quantitative data for wear track width (WTW), wear volume (V), and wear rate (K) are summarized in Table 3.

**Table 3.** Wear analysis for biolubricants.

| Lubricant | WTW (μm) | K ($\times 10^{-7}$ mm$^3$/Nm) | V ($\times 10^{-4}$ mm$^3$) |
|---|---|---|---|
| COSO | 112 ± 13 | 18.4 | 10.0 |
| CSA 1 | 72 ± 7 | 4.68 | 2.65 |
| CSA 2 | 83 ± 8 | 7.34 | 4.15 |
| CSA 3 | 87 ± 7 | 8.18 | 4.63 |

According to the results, the base formulation shows the highest surface degradation, with a wear track width of 112 ± 13 μm, a volume loss of $10 \times 10^{-4}$ mm$^3$, and a wear rate of $18.4 \times 10^{-7}$ mm$^3$/Nm. In contrast, the formulations containing ascorbyl palmitate demonstrate a significant reduction in all evaluated parameters. Specifically, CSA 1 shows a reduction in wear track width of approximately 36% and a decrease in wear rate of about 75% compared to COSO, while CSA 3 exhibits intermediate reductions. These findings confirm the positive effect of a moderate concentration of the additive on the wear resistance of the system.

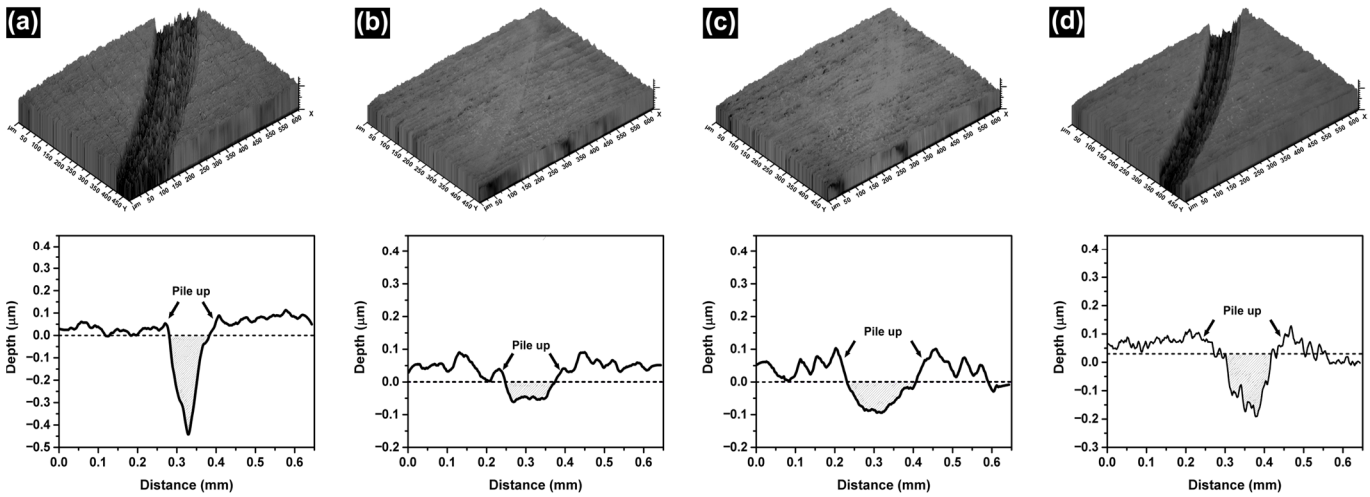


**Figure 8.** Optical 2.5D micrographs at 200× and roughness profile of wear track for (**a**) COSO, (**b**) CSA 1, (**c**) CSA 2, and (**d**) CSA 3.

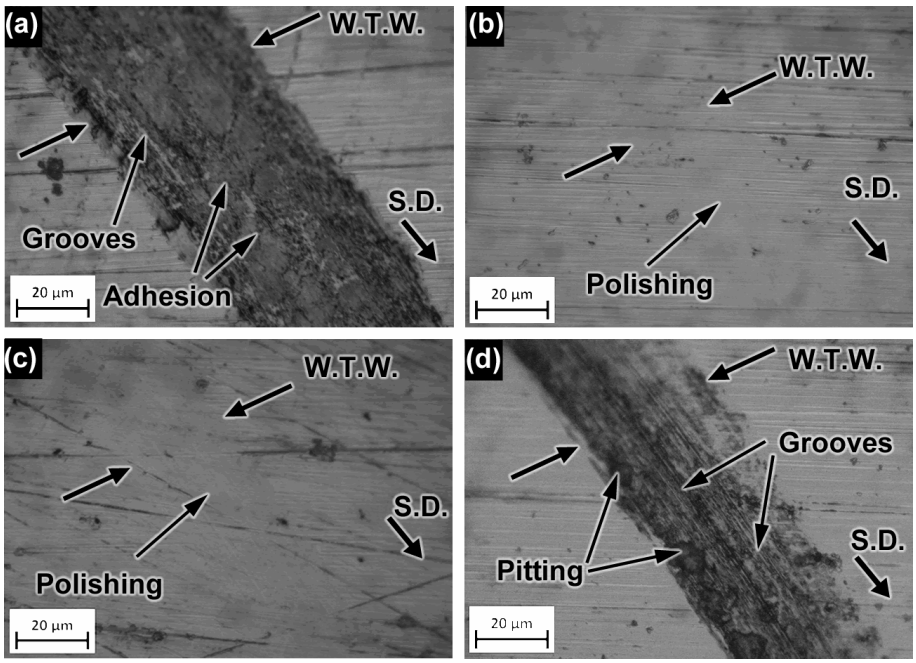


**Figure 9.** Optical micrographs at 500X exhibiting wear mechanisms for (**a**) COSO, (**b**) CSA 1, (**c**) CSA 2, and (**d**) CSA 3.

Similar results have been observed in biolubricants modified with natural additives, where polar compounds help reduce wear by forming protective interfacial layers [32]. In particular, Moreno et al. [35] reported significant improvements in the tribological performance of vegetable oils with natural additives, linked to interfacial interaction mechanisms. Likewise, studies on biolubricants have shown reductions in the wear rate ranging from 40 to 70% when using polar additives, which aligns with the approximately 75% reduction seen for CSA 1 in this work [16,35].

The observed trend in wear values aligns with the previously discussed friction results, where CSA 1 and CSA 2 showed the lowest coefficients of friction. This correlation with polar additives indicates that adsorbed layers reduce both tangential forces and surface damage [16,35,37].

The analysis of 2.5D surface topographies and cross-sectional profiles reveals clear differences in wear mechanisms (Figure 8). In the case of CSA 1 and CSA 2, a relatively

uniform surface is observed, with slight material accumulation (pile-up) at the edges of the wear track and evidence of surface polishing. This behavior is characteristic of mild wear dominated by plastic deformation and surface smoothing.

In contrast, CSA 3 (Figure 8c) displays well-defined grooves, indicating abrasive wear. Although its performance remains better than that of the base formulation, a shift toward more severe wear mechanisms is observed, aligning with the increased friction coefficient. Lastly, COSO (Figure 8d) demonstrates the most advanced wear mechanisms, with deep grooves, substantial material buildup, and areas related to adhesion. This behavior suggests combined adhesive and abrasive wear, consistent with the high $\mu_k$ and wear rate values recorded for this formulation.

From a wear mechanism perspective, these results can be interpreted based on the classification proposed by Kato [28], where abrasive, adhesive, and polishing wear mechanisms are clearly differentiated (Figure 9). Specifically, formulations with low to intermediate concentrations of ascorbyl palmitate encourage mild wear conditions mainly characterized by polishing, while the absence of the additive leads to more severe mechanisms like abrasion and adhesion dominating.

Furthermore, microhardness measurements were taken inside the wear tracks. The AISI 4140 steel showed an initial hardness of 192 HV, while no notable changes were seen in CSA 1 and CSA 2. Conversely, CSA 3 and COSO displayed increased hardness values of 223 and 203 HV, respectively. This increase in hardness likely results from work hardening caused by repeated stresses during sliding, aligning with the more severe wear mechanisms observed in these formulations. Similar wear patterns have been documented in steel–steel contacts under intense conditions, where accumulated plastic deformation raises surface hardness [37].

It is also worth noting that microstructural analysis was performed on the wear track associated with the CSA 3 formulation. As shown in Figure 10, the worn region (region 1) displays a clear refinement of the grain structure compared to the unworn material (region 2). This localized microstructural change indicates severe plastic deformation caused by sliding contact, resulting in grain fragmentation and reorganization. The presence of grain refinement in CSA 3 aligns with the observed increase in hardness and supports the interpretation of deformation-driven wear mechanisms under more severe contact conditions.

Overall, these results show that adding ascorbyl palmitate not only reduces friction but also alters wear mechanisms, encouraging a shift toward less severe tribological conditions at the interface.

### *3.7. Thermal and Oxidation Behavior*

Figure 11 and Table 4 show the thermal and oxidation behavior of biolubricants. It can be observed that COSO begins its decomposition at 256 °C with an 8% mass loss, reaching a degradation peak at 285 °C with a 33% loss. Subsequently, a second event occurs at 347 °C, leaving only 3% residue. This reflects a rapid and almost complete degradation of the triglycerides, with a minimal stable fraction. In contrast, the oil with 0.5 wt.% ascorbyl palmitate (CSA 2) shows a later onset (265 °C) and less initial loss (6%). Its first degradation peak occurs at 288 °C, with a 26% mass loss, followed by a second, broader, and less intense event at 355 °C. The final residue reaches 10%, significantly higher than in COSO. This confirms that ascorbyl palmitate delays decomposition and promotes the formation of a more stable residue, thus reducing the degradation rate in the second stage.

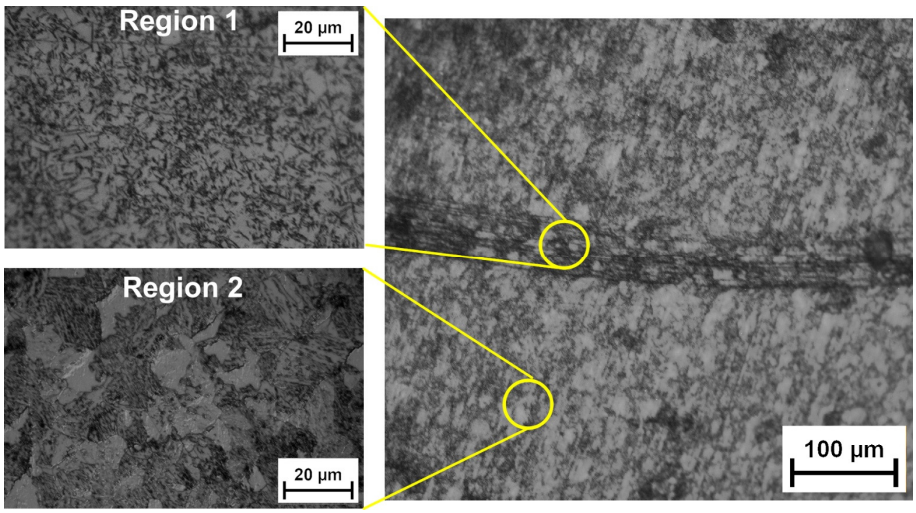


**Figure 10.** Microstructural features of the wear track of AISI 4140 lubricated with CSA 3 showing grain refinement (region 1) compared to the unworn zone (region 2).

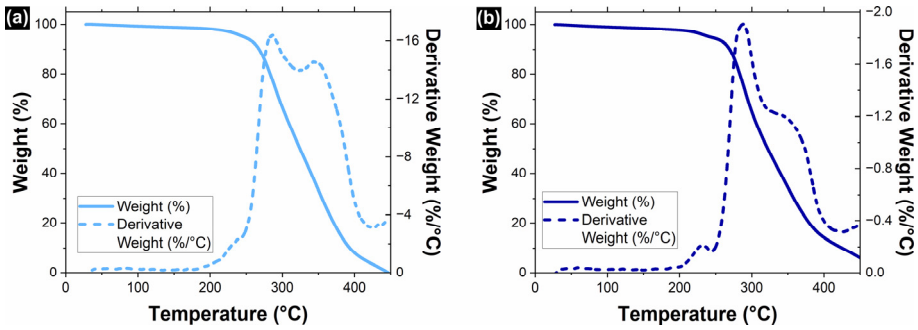


**Figure 11.** TGA-DTG analyses of (**a**) COSO and (**b**) CSA 2.

**Table 4.** Thermal and oxidation behavior of COSO and CSA 2.

| Biolubricant | $T_{onset}$ (°C) | Weight Loss at $T_{onset}$ (%) | Decomposition Temperature Range (°C) | Peak Decomposition Temperature (°C) | Residue (%) | OOT (°C) |
|---|---|---|---|---|---|---|
| COSO | 256 | 8% | 256–319<br>319–386 | 285<br>347 | 3% | 269 |
| CSA 2 | 265 | 6% | 265–330<br>330–400 | 288<br>355 | 10% | 274 |

On the other hand, Table 4 also shows that the pure oil (COSO) has an OOT of 269 °C, while the oil with 0.5 wt.% ascorbyl palmitate (CSA 2) raises it slightly to 274 °C. This shift confirms that the antioxidant additive delays the onset of oxidation, providing greater thermal stability.

Overall, the change in decomposition kinetics and the higher OOT demonstrate that ascorbyl palmitate improves the thermal and oxidative stability of the oil, reduces mass loss during critical stages, and increases the percentage of final residue, thus demonstrating its protective effect against degradation.

## 4. Final Discussion

The results from this study show that the tribological performance of biolubricants formulated with ascorbyl palmitate is not determined by changes in bulk lubricant properties but mainly by interfacial phenomena. Although the differences in viscosity and density

among formulations are small, and the lubricant film thickness remains in the nanometer range, significant improvements in both the coefficient of friction and wear resistance are observed depending on the dosage. This behavior aligns with boundary lubrication literature and the role of polar additives in forming protective adsorbed layers [35,45].

The lubrication regime analysis confirms that all formulations operate under boundary lubrication conditions, indicating incomplete surface separation and predominant asperity interactions. Under these conditions, the enhanced performance of the ascorbyl palmitate-containing formulations cannot be attributed to hydrodynamic effects but rather to the additive's action at the lubricant–surface interface. The presence of an optimum at low-to-intermediate additive concentrations suggests that more effective surface coverage results in a greater reduction in friction and wear, while higher concentrations do not offer a comparable improvement [35,45].

The wear trend aligns with the friction results. The CSA 1 and CSA 2 biolubricants show the lowest $\mu_k$ values and the highest lubrication efficiency, while COSO and CSA 3 exhibit more severe surface damage. Regarding wear mechanisms, the best-performing surfaces display polishing features, whereas the less effective formulations demonstrate abrasive and adhesive wear, as classified by Kato [28]. This change in wear mechanisms is typical of boundary-lubricated systems, where surface chemistry and the adsorption of active species control tribological damage [28].

Microhardness measurements within the wear track and microstructural analysis offer further insight into the nature of the contact. Notably, the hardness increase observed for CSA 3 and COSO, along with grain refinement within the wear track for CSA 3, suggests localized plastic deformation and strain buildup under more intense contact conditions. This behavior is consistent with work hardening seen in steel–steel contacts experiencing severe wear, where repeated deformation causes microstructural changes on the surface [37].

Overall, the correlation between friction, wear, and microhardness indicates that formulations containing ascorbyl palmitate at low-to-intermediate concentrations promote more favorable contact conditions, reducing plastic deformation and limiting the development of severe wear mechanisms. From a functional perspective, this behavior can be explained by the ability of the additive to interact with the metallic surface and form adsorbed layers that reduce direct asperity contact and lower tangential stresses during sliding [35,45,46].

Furthermore, the temporal evolution of the contact angle clarifies the adsorption kinetics of the additive on the metal surface. The modified formulations (CSA) exhibit a drastic reduction in the angle after 75 s, with significant differences between 37.1° and 39.8° compared to the mostly cohesive response of COSO (20.3°). This remarkable surface affinity, governed by the polar and amphiphilic nature of ascorbyl palmitate, directly correlates with the reduced settling period, allowing CSA 1 and CSA 2 to reach steady state in as few as $5 \times 10^3$ cycles. In contrast, the lack of active agents in COSO or the chemically aggressive and disorganized environment of CSA 3 drastically prolongs this transition to $15 \times 10^3$ cycles.

The observed behavior suggests the existence of an optimum ascorbyl palmitate concentration for maximizing the tribological response of the system. CSA1 and CSA2 exhibited the lowest friction and wear values, whereas a further increase in additive concentration (CSA3) did not produce equivalent improvements. This trend is consistent with that reported for polar organic friction modifiers, whose effectiveness is often maximized at intermediate concentrations and does not necessarily increase proportionally with additive content [41,45].

Ascorbyl palmitate possesses an amphiphilic molecular structure consisting of a polar ascorbate moiety and a sixteen-carbon hydrocarbon chain derived from palmitic acid [46]. This molecular configuration enhances its compatibility with oil-based matrices while enabling simultaneous interactions with both the lubricant and the metallic surface. Y. Long et al. [8] demonstrated that ascorbyl palmitate can adsorb onto steel surfaces and act as an effective friction modifier through the formation of protective interfacial films. The authors identified C-O-Fe bonds by XPS analysis and observed, through AFM measurements, the development of a surface layer capable of significantly reducing friction and wear [8].

Under the boundary lubrication conditions identified in this work, even nanometric modifications at the interface can produce substantial changes in tribological behavior. In this regard, the calculated lubricant film thicknesses are of the same order of magnitude as the adsorbed boundary films commonly reported for organic friction modifiers [8,37,46]. Although these values correspond to the total lubricant film thickness rather than a direct measurement of an ascorbyl palmitate-derived layer, this correspondence further supports the hypothesis that interfacial phenomena play a dominant role in the lubrication mechanism observed.

According to Spikes [41], friction reduction in systems lubricated with organic friction modifiers is strongly related to the degree of surface coverage achieved by the adsorbed molecules. As additive concentration increases, surface coverage progressively approaches a maximum value, after which further increases in concentration provide diminishing benefits. Consequently, the superior performance of CSA1 and CSA2 may be associated with more effective surface coverage and the establishment of favorable interfacial conditions that reduce direct asperity contact. Conversely, the behavior observed for CSA3 suggests that increasing the ascorbyl palmitate concentration beyond 0.5 wt.% does not lead to a proportional improvement in tribological performance, which is consistent with the behavior reported for other adsorptive friction modifiers [41,46]. Overall, these findings suggest the existence of an optimum concentration window for ascorbyl palmitate in the castor oil–sesame oil binary molar mixture employed in this study.

Finally, the tribological conditions and lubricant properties evaluated in this study, including a viscosity range consistent with ISO VG 150, SAE 40, AGMA 4, and SUS 650N lubricant grades, according to the viscosity grade equivalence reported by Mang et al. [47], are representative of those encountered in heavily loaded steel–steel contacts commonly found in rolling/sliding elements, cam-follower systems, and other power-transmission components [37,47,48]. These systems frequently operate under contact pressures ranging from several hundred MPa to the GPa range [37,47,48]. In this context, the reductions in friction and wear achieved by CSA1 and CSA2, together with their improved lubrication efficiency, suggest that these formulations have potential for use as biodegradable alternatives for applications requiring effective surface protection under severe operating conditions.

## 5. Conclusions

The results of this study show that adding ascorbyl palmitate to a binary molar mixture of castor and sesame oils significantly improves the system's tribological performance. A summary of the highlights is as follows:

- The formulation CSA 1 showed the best overall performance, reducing the steady-state coefficient of friction by about 50% and the wear rate by up to 75% compared to the base formulation.
- CSA 1 and CSA 2 exhibited higher lubrication efficiency and reached steady-state conditions in fewer cycles, whereas CSA 3, despite showing a reduced coefficient of friction, did not significantly affect the stabilization time.

- The physicochemical characterization showed differences below 5% in density and viscosity among formulations, confirming that the observed improvements are not linked to major changes in bulk rheological properties.
- The lubrication regime analysis revealed that all systems operated under boundary lubrication conditions, with film thickness values ranging from 2.6 to 4.1 nm, which are not enough to ensure complete surface separation.
- Wear analysis showed that CSA 1 and CSA 2 caused milder wear mainly through surface polishing, while COSO and CSA 3 exhibited more severe wear, such as abrasion and adhesion.

Overall, the results show that the enhanced performance of CSA 1 mainly depends on interfacial phenomena, especially the additive's ability to lower asperity interactions under boundary lubrication conditions.

Future work should focus on surface characterization using X-ray photoelectron spectroscopy (XPS) and complementary techniques to examine the potential formation of tribochemical layers, including species derived from iron and ascorbyl palmitate, such as iron–ascorbate compounds, to better understand the interfacial mechanisms behind the observed tribological improvements.

**Author Contributions:** Conceptualization, K.J.M. and M.T.H.-S.; formal analysis, K.J.M., M.T.H.-S. and J.E.B.; investigation, S.R.-O. and M.U.N.-R.; methodology, S.R.-O. and M.U.N.-R.; validation, K.J.M., M.T.H.-S. and J.E.B.; writing—original draft, S.R.-O. and M.U.N.-R.; writing—review and editing, K.J.M. and M.T.H.-S.; funding acquisition, K.J.M. and M.T.H.-S. All authors have read and agreed to the published version of the manuscript.

**Funding:** This research was funded by Tecnológico Nacional de México (TecNM), project number 25321.26-PD.

**Data Availability Statement:** The data presented in this study are available upon request from the corresponding author.

**Acknowledgments:** The authors acknowledge Tecnológico Nacional de México (TecNM) for its support with the projects CELA-PYR-2026-24486 and 25321.26-PD. S.R.-O. and M.U.N.-R. acknowledge the Secretaría de Ciencia, Humanidades, Tecnología en Innovación (Secihti) in Mexico for the grant for doctoral studies.

**Conflicts of Interest:** The authors declare no conflicts of interest.

## References

1. Patel, J.R.; Chauhan, K.V.; Rawal, S.; Patel, N.P.; Subhedar, D. Advances and Challenges in Bio-Based Lubricants for Sustainable Tribological Applications: A Comprehensive Review of Trends, Additives, and Performance Evaluation. *Lubricants* **2025**, *13*, 440. [CrossRef]
2. Berman, D. Plant-Based Oils for Sustainable Lubrication Solutions—Review. *Lubricants* **2024**, *12*, 300. [CrossRef]
3. Ortega-Álvarez, R.; Hernández-Sierra, M.T.; Aguilera-Camacho, L.D.; Bravo-Sánchez, M.G.; Moreno, K.J.; García-Miranda, J.S. Tribological Performance of 100Cr6/8620 Steel Bearing System under Green Oil Lubrication. *Metals* **2022**, *12*, 362. [CrossRef]
4. Minami, I. Molecular Science of Lubricant Additives. *Appl. Sci.* **2017**, *7*, 445. [CrossRef]
5. Prasannakumar, P.; Sankarannair, S.; Prasad, G.; Krishna, H.; Pranav, S.; Vivek, P.; Sidharth, S.; Shanmugam, R. Bio-based additives in lubricants: Addressing challenges and leveraging for improved performance toward sustainable lubrication. *Biomass Convers. Biorefin.* **2025**, *15*, 17969–17997. [CrossRef]
6. Abdouli, A.; Djebbi, M.A.; Haj Amara, A.B. Synergistic corrosion inhibition and controlled release of ascorbic acid from a layered double hydroxide composite for stainless steel. *J. Electrochem. Sci. Eng.* **2025**, *15*, 2808. [CrossRef]
7. Hancock, R.D.; Viola, R. Biotechnological approaches for l-ascorbic acid production. *Trends Biotechnol.* **2002**, *20*, 299. [CrossRef] [PubMed]
8. Long, Y.; Martin, J.M.; Dubreuil, F.; Thiebaut, B.; Loehle, S.; Lacassagne, C.; De Barros Bouchet, M.-I. Ascorbyl Palmitate-Vitamin C Effective Friction Modifier and Wear Inhibitor for Steel in a PAO Base Oil. *Lubricants* **2022**, *10*, 253. [CrossRef]

9. Ruger, C.W.; Klinker, E.J.; Hammond, E.G. Abilities of some antioxidants to stabilize soybean oil in industrial use conditions. *J. Am. Oil Chem. Soc.* **2002**, *79*, 733–736. [CrossRef]
10. González, M.; Gallego, R.; Romero, M.A.; González-Delgado, J.A.; Arteaga, J.F.; Valencia, C.; Franco, J.M. Impact of natural sources-derived antioxidants on the oxidative stability and rheological properties of castor oil based-lubricating greases. *Ind. Crops Prod.* **2016**, *87*, 297–303. [CrossRef]
11. Moolayil, J.T.; Aravind, A.; Sasikumar, S.K. Study on Physicochemical, Rheological and Oxidative Properties of RSO with Suitable Additives. *AIP Conf. Proc.* **2019**, *2134*, 050003. [CrossRef]
12. Quinchia, L.A.; Delgado, M.A.; Valencia, C.; Franco, J.M.; Gallegos, C. Natural and Synthetic Antioxidant Additives for Improving the Performance of New Biolubricant Formulations. *J. Agric. Food Chem.* **2011**, *59*, 12917–12924. [CrossRef] [PubMed]
13. Hernández-Sierra, M.T.; Aguilera-Camacho, L.D.; Báez-García, J.E.; García-Miranda, J.S.; Moreno, K.J. Thermal Stability and Lubrication Properties of Biodegradable Castor Oil on AISI 4140 Steel. *Metals* **2018**, *8*, 428. [CrossRef]
14. Korkmaz, M.E.; Kumar Gupta, M.; Demirsöz, R. Understanding the lubrication regime phenomenon and its influence on tribological characteristics of additively manufactured 316 Steel under novel lubrication environment. *Tribol. Int.* **2022**, *173*, 107686. [CrossRef]
15. Magazov, N.; Satbaeva, Z.; Rakhadilov, B.; Amanov, A. A Study on Surface Hardening and Wear Resistance of AISI 52100 Steel by Ultrasonic Nanocrystal Surface Modification and Electrolytic Plasma Surface Modification Technologies. *Materials* **2023**, *16*, 6824. [CrossRef] [PubMed]
16. Shahidi, F.; Zhong, Y. Lipid oxidation and improving the oxidative stability. *Chem. Soc. Rev.* **2010**, *39*, 4067. [CrossRef] [PubMed]
17. *ASTM D 1217*; Standard Test Method for Density and Relative Density (Specific Gravity) of Liquids by Bingham Pycnometer. ASTM International: West Conshohocken, PA, USA, 1993.
18. *ASTM D 445*; Standard Test Method for Kinematic Viscosity of Transparent and Opaque Liquids (and Calculation of Dynamic Viscosity). ASTM International: West Conshohocken, PA, USA, 2024.
19. Seeton, C.J. Viscosity–temperature correlation for liquids. *Tribol. Lett.* **2006**, *22*, 67. [CrossRef]
20. Saraswat, A.; Bhattacharyay, R.; Chaudhuri, P.; Gedupudi, S. Development of a Test Bed to Investigate Wetting Behaviours of High-Temperature Heavy Liquid Metals for Advanced Nuclear Applications. *Liquids* **2025**, *5*, 33. [CrossRef]
21. *ASTM D 7490: 2022*; Standard Test Method for Measurement of the Surface Tension of Solid Coatings, Substrates and Pigments using Contact Angle Measurements. ASTM International: West Conshohocken, PA, USA, 2022.
22. Ponomar, M.; Krasnyuk, E.; Butylskii, D.; Nikonenko, V.; Wang, Y.; Jiang, C.; Xu, T.; Pismenskaya, N. Sessile Drop Method: Critical Analysis and Optimization for Measuring the Contact Angle of an Ion-Exchange Membrane Surface. *Membranes* **2022**, *12*, 765. [CrossRef] [PubMed]
23. Hamrock, B.J.; Dowson, D. Isothermal elastohydrodynamic lubrication of point contacts: Part III—Fully flooded results. *J. Lubr. Technol.* **1977**, *99*, 264–275. [CrossRef]
24. Hernández-Sierra, M.T.; Bravo-Sánchez, M.G.; Báez, J.E.; Aguilera-Camacho, L.D.; García-Miranda, J.S.; Moreno, K.J. Improvement Effect of Green Lubricants on the Tribological and Mechanical Performance of 4140 Steel. *Appl. Sci.* **2019**, *9*, 4896. [CrossRef]
25. *ASTM G 99*; Standard Test Method for Wear and Friction Testing with a Pin-on-Disk or Ball-on-Disk Apparatus. ASTM International: West Conshohocken, PA, USA, 2023.
26. Ciulli, E.; Betti, A.; Forte, P. The Applicability of the Hertzian Formulas to Point Contacts of Spheres and Spherical Caps. *Lubricants* **2022**, *10*, 233. [CrossRef]
27. Trzepieciński, T.; Szewczyk, M.; Szwajka, K. The Use of Non-Edible Green Oils to Lubricate DC04 Steel Sheets in Sheet Metal Forming Process. *Lubricants* **2022**, *10*, 210. [CrossRef]
28. Kato, K. Classification of Wear Mechanisms/Models. In *Wear—Materials, Mechanisms and Practice*; Stachowiak, G.W., Ed.; John Wiley & Sons Ltd.: West Sussex, UK, 2005; Volume 1, pp. 9–20.
29. Yadav, M.G.; Kavadia, M.R.; Vadgama, R.N.; Odaneth, A.A.; Lali, A.M. Production of 6-O-l-Ascorbyl Palmitate by Immobilized Candida antarctica Lipase B. *Appl. Biochem. Biotechnol.* **2018**, *184*, 1168–1186. [CrossRef] [PubMed]
30. Fadzlillah, N.A.; Che Man, Y.B.; Rohman, A. FTIR Spectroscopy Combined with Chemometric for Analysis of Sesame Oil Adulterated with Corn Oil. *Int. J. Food Prop.* **2014**, *17*, 1275. [CrossRef]
31. Coates, J. Interpretation of Infrared Spectra, A Practical Approach. In *Encyclopedia of Analytical Chemistry*; Meyers, R.A., Ed.; John Wiley & Sons Ltd.: West Sussex, UK, 2000; Volume 1, pp. 10815–10837.
32. Shen, W.; Hirayama, T.; Yamashita, N.; Adachi, M.; Oshio, T.; Tsuneoka, H.; Tagawa, K.; Yagishita, K.; Yamada, N.L. Relationship between interfacial adsorption of additive molecules and reduction of friction coefficient in the organic friction modifiers-ZDDP combinations. *Tribol. Int.* **2022**, *167*, 107365. [CrossRef]
33. Hamrock, B.J.; Schmid, S.R.; Jacobson, B.O. *Fundamentals of Fluid Film Lubrication*, 2nd ed.; CRC Press: Boca Raton, FL, USA, 2004.
34. Mobarak, H.M.; Mohamad, E.N.; Masjuki, H.H.; Kalam, M.A.; Al Mahmud, K.A.H.; Habibullah, M.; Ashraful, A.M. The prospects of biolubricants as alternatives in automotive applications. *Renew. Sustain. Energy Rev.* **2014**, *33*, 34–43. [CrossRef]

35. Moreno, K.J.; Hernández-Sierra, M.T.; Báez, J.E.; Rodríguez-deLeón, E.; Aguilera-Camacho, L.D.; García-Miranda, J.S. On the Tribological and Oxidation Study of Xanthophylls as Natural Additives in Castor Oil for Green Lubrication. *Materials* **2021**, *14*, 5431. [CrossRef] [PubMed]
36. Bhushan, B. *Introduction to Tribology*; Wiley: Hoboken, NJ, USA, 2013.
37. Hutchings, I.; Shipway, P. *Tribology: Friction and Wear of Engineering Materials*, 2nd ed.; Butterworth-Heinemann: Woburn, MA, USA, 2017.
38. Spikes, H. Friction Modifier Additives. *Tribol. Lett.* **2015**, *60*, 5. [CrossRef]
39. Zhu, D.; Wang, Q.J. On the λ ratio range of mixed lubrication. *Proc. Inst. Mech. Eng. Part J J. Eng. Tribol.* **2012**, *226*, 1010–1022. [CrossRef]
40. Keno, W.D.; Kalácska, Á.; Fauconnier, D.; Ancha, V.R.; De Baets, P. An Experimental Investigation of the Impact of Additive Concentration on the Tribological Performance of Castor Oil Lubrication in Piston Ring–Cylinder Liner Contact. *Lubricants* **2025**, *13*, 206. [CrossRef]
41. Marmorat, T.; Wijanarko, W.; Espallargas, N.; Khanmohammadi, H. Effect of the Polar Head Type on the Surface Adsorption and Tribofilm Formation of Organic Friction Modifiers in Water-Based Lubricants. *Langmuir* **2024**, *40*, 7920–7932. [CrossRef] [PubMed]
42. Spikes, H. Mechanisms of ZDDP—An Update. *Tribol. Lett.* **2025**, *73*, 38. [CrossRef]
43. Cosimbescu, L.; Robinson, J.W.; Zhou, Y.; Qu, Y. Dual functional star polymers for lubricants. *RSC Adv.* **2016**, *6*, 86259–86268. [CrossRef]
44. Johnson, K.L. *Contact Mechanics*; Cambridge University Press: Cambridge, UK, 1985.
45. Spikes, H. The History and Mechanisms of ZDDP. *Tribol. Lett.* **2004**, *17*, 469–489. [CrossRef]
46. Rowe, R.C.; Sheskey, P.J.; Quinn, M.E. *Handbook of Pharmaceutical Excipients*, 6th ed.; Pharmaceutical Press and American Pharmacists Association: London, UK, 2009.
47. Dresel, W.; Mang, T. (Eds.) *Lubricants and Lubrication*, 3rd ed.; Wiley-VCH: Weinheim, Germany, 2017.
48. Harris, T.A.; Kotzalas, M.N. *Rolling Bearing Analysis*, 5th ed.; CRC Press: Boca Raton, FL, USA, 2007.


**Disclaimer/Publisher's Note:** The statements, opinions and data contained in all publications are solely those of the individual author(s) and contributor(s) and not of MDPI and/or the editor(s). MDPI and/or the editor(s) disclaim responsibility for any injury to people or property resulting from any ideas, methods, instructions or products referred to in the content.